Supporting Information for

Campylobacter jejuni KDO8P Synthase, its Inhibition by KDO8P Oxime, and Control of the Residence Time of Slow-binding Inhibition

*Simanga R. Gama,[1] Naresh Balachandran,[1] and Paul J. Berti[1,2,]**

[1]Department of Chemistry & Chemical Biology and [2]Department of Biochemistry & Biomedical Sciences, McMaster University, 1280 Main St. W., Hamilton, Ontario L8S 4M1, Canada

* Author to whom correspondence should be addressed.

E-mail: berti@mcmaster.ca

Table of Contents

Table S1. Primer sequences.

Name	Primer sequence
	Gateway cloning [a]
Forward	5′ – GGGG ACA AGT TTG TAC AAA AAA GCA GGC TTC **GAA AAC CTG TAT TTT CAG GGC** *ATG AAA AAA ATG ATA CTC ATT GCT GGT CC* – 3′
Reverse	5′ - GGG GAC CAC TTT GTA CAA GAA AGC TGG GTC *TTA TTT GTT TTC CTT TAT GAT ATT TTG TAT TTC* – 3′
	Stop codon removal [b]
Forward	5′ – *CATAAAGGAAAACAAA*TAACATCACCATCACCATCAC – 3′
Reverse	5′ – GTGATGGTGATGGTGATGTTATT*TGTTTTCCTTTATG* – 3′

[a] Underline = attB restriction site, bold = TEV protease cleavage site, italics = KDO8PS gene

[b] Underline = stop codon, italics = KDO8PS gene

```
atgaaaaaaatgatactcattgctggtccttgcgtgatagaaagcaaagatttgatttttt
 M  K  K  M  I  L  I  A  G  P  C  V  I  E  S  K  D  L  I  F
aaagttgctgaacagttaaaaaatttttaatgaaaatccaaatatagaattttatttcaaa
 K  V  A  E  Q  L  K  N  F  N  E  N  P  N  I  E  F  Y  F  K
tcaagttttgataaggccaatcgcacaagtattaattcttttcgaggtcctggtcttgaa
 S  S  F  D  K  A  N  R  T  S  I  N  S  F  R  G  P  G  L  E
gaaggattaaaaattttacaaagcgtaaaagatgaatttggtatgaaaatcttaaccgat
 E  G  L  K  I  L  Q  S  V  K  D  E  F  G  M  K  I  L  T  D
atacacgaaagcaatcaagcaaaccctgtaagtgaagtagctgatgtcttgcaaattcct
 I  H  E  S  N  Q  A  N  P  V  S  E  V  A  D  V  L  Q  I  P
gctttttatgtcgtcaaaccgatttacttgtagccgcagcaaaaactaaggcaaaaatt
 A  F  L  C  R  Q  T  D  L  L  V  A  A  A  K  T  K  A  K  I
aatatcaaaaaaggacaatttttaaacccaagcgatatcaaatacagcgttaaaaaagtt
 N  I  K  K  G  Q  F  L  N  P  S  D  I  K  Y  S  V  K  K  V
ctacaaacccgtggtatagaagatgaaggctatgaagctgctcaaagaaatggtgttttt
 L  Q  T  R  G  I  E  D  E  G  Y  E  A  A  Q  R  N  G  V  F
gtagctgaaagaggggctagctttggctatggaaatttagtagtagatatgcgttcttta
 V  A  E  R  G  A  S  F  G  Y  G  N  L  V  V  D  M  R  S  L
gttatcatgcgtgaatttgctccagttatttttgatgctacccatagcgtacaaatgcca
 V  I  M  R  E  F  A  P  V  I  F  D  A  T  H  S  V  Q  M  P
ggggctgcaggtggaagtagcggagggaaaagcgaatttgtagaacctttagcaagagcg
 G  A  A  G  G  S  S  G  G  K  S  E  F  V  E  P  L  A  R  A
gcagcagccgtaggcatagatggctttttctttgaaacacatattaatccttgcgaggct
 A  A  A  V  G  I  D  G  F  F  F  E  T  H  I  N  P  C  E  A
ttatgcgatggacctaatatgcttaatcttacacgccttaaaaattgcgttaatacatta
 L  C  D  G  P  N  M  L  N  L  T  R  L  K  N  C  V  N  T  L
ctagaaatacaaaatatcataaaggaaaacaaataa
 L  E  I  Q  N  I  I  K  E  N  K  -
```

Figure S1. Sequence of wild type *C. jejuni* KDO8PS (KDO8PS$_{wt}$).
The *C*-terminal hexa-histidine tag was removed by introducing a stop codon, TAA (green text) before the His$_6$-tag sequence.

atgcatcatcatcatcatcacatcacaagtttgtacaaaaaagcaggcttcgaaaacctg
M H H H H H H I T S L Y K K A G F E N L
tattttcagggcatgaaaaaaatgatactcattgctggtccttgcgtgatagaaagcaaa
Y F Q G M K K M I L I A G P C V I E S K
gatttgatttttaaagttgctgaacagttaaaaaatttttaatgaaaatccaaatatagaa
D L I F K V A E Q L K N F N E N P N I E
ttttatttcaaatcaagttttgataaggccaatcgcacaagtattaattcttttcgaggt
F Y F K S S F D K A N R T S I N S F R G
cctggtcttgaagaaggattaaaaattttacaaagcgtaaaagatgaatttggtatgaaa
P G L E E G L K I L Q S V K D E F G M K
atcttaaccgatatacacgaaagcaatcaagcaaaccctgtaagtgaagtagctgatgtc
I L T D I H E S N Q A N P V S E V A D V
ttgcaaattcctgctttttatgtcgtcaaaccgatttacttgtagccgcagcaaaaact
L Q I P A F L C R Q T D L L V A A A K T
aaggcaaaaattaatatcaaaaaaggacaatttttaaacccaagcgatatcaaatacagc
K A K I N I K K G Q F L N P S D I K Y S
gttaaaaaagttctacaaacccgtggtatagaagatgaaggctatgaagctgctcaaaga
V K K V L Q T R G I E D E G Y E A A Q R
aatggtgtttttgtagctgaaagaggggctagctttggctatggaaatttagtagtagat
N G V F V A E R G A S F G Y G N L V V D
atgcgttctttagttatcatgcgtgaatttgctccagttatttttgatgctacccatagc
M R S L V I M R E F A P V I F D A T H S
gtacaaatgccaggggctgcaggtggaagtagcggagggaaaagcgaatttgtagaacct
V Q M P G A A G G S S G G K S E F V E P
ttagcaagagcggcagcagccgtaggcatagatggctttttctttgaaacacatattaat
L A R A A A A V G I D G F F F E T H I N
ccttgcgaggctttatgcgatggacctaatatgcttaatcttacacgccttaaaaattgc
P C E A L C D G P N M L N L T R L K N C
gttaatacattactagaaatacaaaatatcataaaggaaaacaaataa
V N T L L E I Q N I I K E N K -

Figure S2. Sequence of His$_6$-tagged *C. jejuni* KDO8PS (KDO8PS$_{H6}$).
The *N*-terminal hexahistidine tag is shown in blue text. TEV protease recognizes the ENLYFQG recognition site (red text) and cleaves at the Gln↑Gly (Q↑G) bond (underlined).

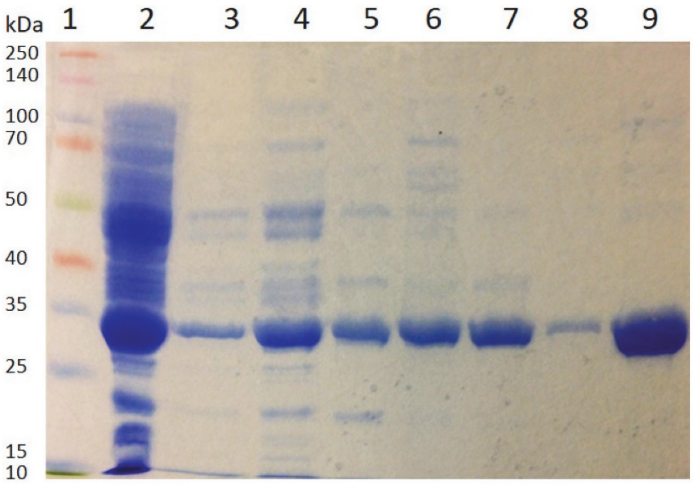

Figure S3. 13% SDS-PAGE gel of KDO8PS$_{wt}$.
Lanes: 1) Molecular weight standards ladder; 2) cell lysate; 3) 0 - 60% $(NH_4)_2SO_4$ fractionation supernatant; 4) 60 - 80% $(NH_4)_2SO_4$ fractionation pellet; 5) Phenyl Sepharose fraction; 6) Q-Sepharose anion exchange purification; 7, 8, 9) Size exclusion chromatography.

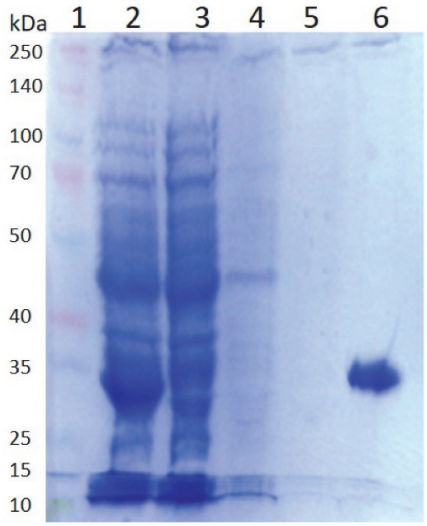

Figure S4. 13% SDS-PAGE gel of KDO8PS$_{H6}$.
Lanes: 1) Molecular weight standards ladder; 2) lysate; 3) column flow-through; 4) buffer A wash; 5) 10 % buffer B wash; 6) Pure fraction eluted at 80 % buffer B.

Table S2. Dynafit models of the steady state kinetic mechanisms.

A = Mn^{2+}, B = PEP, C = A5P, P = KDO8P, Q = P_i. All concentration units are μM and time units are s^{-1}. Association rate constants have units of μM^{-1} s^{-1}.

"Random A" kinetic mechanism

```
[task]
      task = fit
      data = rates
      approximation = king-altman
model random A, ordered B, C

[reaction]

A + B + C ==> APQ

[mechanism]

reaction A + B + C ==> APQ
E + A     <==>  EA           :     k1    k-1
EA + B    <==>  EAB          :     k2    k-2
EAB + C   <==>  EABC         :     k3    k-3
EABC       ==>  E + APQ      :     k4
E + B     <-->  EB           :     k5    k-5
EB + A    <-->  EAB          :     k6    k-6
EB + C    <-->  EBC          :     k7    k-7
EBC + A   <-->  EABC         :     k8    k-8

[constants]
k1    = 10
k-1   = 3162  ?
k2    = 0.1
k-2   = 5.2  ?
k3    = 10
k-3   = 435  ?
k4    = 2.5  ?
k5    = 0.1
k-5   = (k5 k-2 k-1 k6) / (k2 k1 k-6)
k6    = 1
k-6   = 6.5  ?
k7    = 1000
k-7   = (k7 k-3 k-6 k8) /  (k6 k-8 k3)
k8    = 1000
k-8   = 4910  ?
```

Ordered kinetic mechanism

```
[task]
      task = fit
      data = rates
      approximation = king-altman
model sequential ordered steady-state ter ter

[reaction]

A + B + C ==> APQ
```

```
[mechanism]

reaction A + B + C ==> APQ
  E + A <==> EA              :      k1    k-1
  EA + B <==> EAB            :      k2    k-2
  EAB + C <==> EABC          :      k3    k-3
  EABC ==> E + APQ           :      k4

[constants]
k1    = 10
k-1   = 1323.89  ?
k2    = 1
k-2   = 574.843  ?
k3    = 1000
k-3   = 21038.1  ?
k4    = 2.37612  ?
```

Table S3. Microscopic rate constants for the steady state "random A" sequential ter ter kinetic mechanism for KDO8PS$_{wt}$.
After two rounds of initial scans and optimization, the five best sets of initial estimates were optimized (Figure 2.5). The initial estimates of the association rate constants (k_1, $k_{2,}$…) were fixed, while the dissociation rate constants (k_{-1}, $k_{-2,}$…), and k_{cat} (k_4) were optimized. A = Mn^{2+}, B = PEP, C = A5P.

Model #	Random A 195	Random A 146	Random A 367	Random A 373	Random A 234	Random A 212
k_1 ($\mu M^{-1}s^{-1}$)	10	10	10	10	10	
k_{-1} (s^{-1})	$(0.03 \pm 9.90) \times 10^5$	$(0.012 \pm 127) \times 10^4$	$(0.012 \pm 130) \times 10^4$	$(0.3 \pm 252) \times 10^4$	$(0.01 \pm 134) \times 10^4$	$(0.1 \pm 47) \times 10^2$
k_2 ($\mu M^{-1}s^{-1}$)	0.1	0.1	0.1	0.1	0.1	0.1
k_{-2} (s^{-1})	5 ± 439	7 ± 1016	7 ± 1029	5 ± 1198	7 ± 1079	7 ± 14
k_3 ($\mu M^{-1}s^{-1}$)	10	10	10	10	1000	10
k_{-3} (s^{-1})	$(0.4 \pm 3.9) \times 10^3$	$(0.4 \pm 8.5) \times 10^3$	$(0.4 \pm 8.6) \times 103$	$(0.04 \pm 1.10) \times 10^4$	$(0.4 \pm 9.1) \times 10^5$	419 ± 163
k_4 (s^{-1})	2.5 ± 0.5	2.5 ± 1.1	2.5 ± 1.2	2.5 ± 1.4	2.5 ± 1.2	2.5 ± 0.1
k_5 ($\mu M^{-1}s^{-1}$)	0.1	0.1	0.1	0.1	0.1	0.01
k_{-5} (s^{-1})[a]	252	1.9	2	142	1.3	0.0089
k_6 ($\mu M^{-1}s^{-1}$)	1	1	0.1	0.1	1	1
k_{-6} (s^{-1})	7 ± 8797	$(0.04 \pm 21) \times 10^3$	4 ± 2100	1 ± 2332	$(0.04 \pm 22) \times 10^3$	45 ± 159
k_7 ($\mu M^{-1}s^{-1}$)	1000	10	10	1000	1000	10
k_{-7} (s^{-1})[b]	5.8×10^4	4.4×10^3	4.4×10^3	9.3×10^4	4.5×10^5	4.9×10^3
k_8 ($\mu M^{-1}s^{-1}$)	1000	1000	1000	1000	1000	1000
k_{-8} (s^{-1})	$(0.05 \pm 2) \times 10^5$	$(0.4 \pm 5) \times 10^5$	$(0.4 \pm 5) \times 10^5$	$(0.5 \pm 6) \times 10^5$	$(0.4 \pm 5) \times 10^5$	$(3.8 \pm 4.4) \times 10^3$
Derived kinetic constants						
k_{cat} (s^{-1}) (= k_4)	2.5 ± 0.5	2.5 ± 1.1	2.5 ± 1.2	2.5 ± 1.4	2.5 ± 1.2	2.5 ± 0.1
K_d,A (μM) (= k_{-1}/k_1)	$(0.03 \pm 9.9) \times 10^5$	$(0.001 \pm 1.3) \times 10^5$	$(0.001 \pm 1.3) \times 10^5$	$(0.03 \pm 2.5) \times 10^5$	$(0.03 \pm 2.5) \times 10^5$	$8 \pm (1.5 \times 10^5)$
K_d,B (μM) (= k_{-2}/k_2)	52 ± 4388	$(0.07\pm 10) \times 10^3$	$(0.07\pm 10) \times 10^3$	$(0.05\pm 12) \times 10^3$	$(0.07\pm 11) \times 10^3$	70 ± 137
K_d,C (μM) (= k_{-3}/k_3)	44 ± 395	42 ± 848	42 ± 862	43± 1097	42± 908	42 ±16
(k_{-5}/k_5) (μM)	2515	19	20	1425	13	0.89
(k_{-6}/k_6) (μM)	$(0.1\pm 88) \times 10^2$	$(0.4\pm 207) \times 10^2$	$(0.1\pm 233) \times 10^2$	$(0.4\pm 220) \times 10^2$	$(0.4\pm 218) \times 10^2$	45 ± 159
k_{-7}/k_7) (μM)	58	444	444	93	452	488
k_{-8}/k_8) (μM)	5 ± 212	4 ± 460	4 ± 468	5 ± 578	4 ± 490	3.8 ± 4.4

[a] Redundant parameter, calculated as $k_{-5} = (k_5\ k_{-2}\ k_{-1}\ k_6) / (k_2\ k_1\ k_{-6})$. The standard error was not calculated.

[b] Redundant parameter, calculated as $k_{-7} = (k_7\ k_{-3}\ k_{-6}\ k_8) / (k_6\ k_{-8}\ k_3)$. The standard error was not calculated.

Table S4. Microscopic rate constants and King-Altman parameters for the steady state ordered sequential ter ter kinetic mechanism for $KDO8PS_{wt}$.

From the 4050 sets of initial conditions (see main text), the top 500 were fully optimized, and the top 100 results yielded the same six sets of optimized parameters multiple times. Thus, each solution set represents multiple optimizations to the same final parameters.

Solution set number	#1	#2	#3	#4	#5	#6
k_1 ($\mu M^{-1}s^{-1}$)	1000	10	1	1	1	1
k_{-1} (s^{-1})	$(2.5 \pm 0.8) \times 10^5$	$(2.4 \pm 0.8) \times 10^3$	170 ± 70	80 ± 42	70 ± 40	70 ± 40
k_2 ($\mu M^{-1}s^{-1}$)	0.1	0.1	0.1	1	10	1000
k_{-2} (s^{-1})	1 ± 4	1.2 ± 4.0	3 ± 5	660 ± 520	7 ± 6	7 ± 6
k_3 ($\mu M^{-1}s^{-1}$)	0.1	1000	1000	1000	1	1
k_{-3} (s^{-1})	2 ± 1	$(4.8 \pm 1.1) \times 10^4$	$(4.7 \pm 1.1) \times 10^4$	$(2.1 \pm 1.2) \times 10^4$	15 ± 12	15 ± 12
k_4 (s^{-1})	2.5 ± 0.1	2.5 ± 0.1	2.5 ± 0.1	2.4 ± 0.1	2.4 ± 0.1	2.4 ± 0.1
Derived kinetic constants [a]						
k_{cat} (s^{-1})	2.5 ± 0.1	2.5 ± 0.1	2.5 ± 0.1	2.4 ± 0.1	2.4 ± 0.1	2.4 ± 0.1
$K_{M,Mn}$(ss) (μM)	$(3 \pm 0.1) \times 10^{-3}$	0.3 ± 0.01	3 ± 0.1	0.2 ± 0.1	0.2 ± 0.1	0.2 ± 0.1
$K_{M,PEP}$(ss) (μM)	25 ± 1	25 ± 1	25 ± 1	2.0 ± 0.1	2.00 ± 0.01	$(2 \pm 0.1) \times 10^{-3}$
$K_{M,A5P}$(ss) (μM)	49 ± 10	48 ± 11	47 ± 11	21 ± 12	17 ± 12	17 ± 12
$K_{i,Mn}$(ss) (μM)	250 ± 80	240 ± 80	170 ± 70	17 ± 12	140 ± 40	70 ± 40
$K_{i,PEP}$(ss) (μM)	10 ± 40	10 ± 40	30 ± 50	580 ± 520	930 ± 820	970 ± 870
$K_{i,A5P}$(ss) (μM)	20 ± 9	24 ± 11	60 ± 11	5090 ± 12	67560 ± 12	686310 ± 12

[a] The derived kinetic constants are calculated as:[41] $k_{cat} = k_4$, $K_{M,Mn}(ss) = k_4/k_1$, $K_{M,PEP}(ss) = k_4/k_2$, $K_{M,A5P}(ss) = (k_4 + k_{-3})/k_3$, $K_{i,Mn}(ss) = k_{-1}/k_1$, $K_{i,PEP}(ss) = k_{-2}/k_2$, $K_{i,A5P}(ss) = k_{-2}(k_4 + k_{-3})/k_3k_4$.

Table S5. Purification of wild type KDO8PS.

The purification involved ammonium sulphate precipitation, hydrophobic interaction chromatography on Phenyl-Sepharose, anion exchange chromatography on Q-Sepharose, and size exclusion chromatography on Superose 12.

Fraction	Protein (mg)	Specific activity (s^{-1}) [a]	Activity Yield (%) [b]	Purification (fold)
Cell lysate	166	1.1	100	1
60 % ammonium sulphate fractionation	50	2.1	58	2
80 % ammonium sulphate fractionation	34	3.1	58	3
Hydrophobic Chromatography	18	5	49	5
Anion Exchange Chromatography	13	4	28	4
Size exclusion Chromatography	5	2.1 [c]	6	2

[a] Specific activity was measured with the Malachite green/ammonium molybdate assay and the concentration of the enzyme was measured with the Pierce™ BCA Protein Assay Kit (Thermo Scientific).

[b] Activity yield = specific activity × protein × 100%

[c] The specific activity after size exclusion chromatography decreased 2-fold lower relative to the preceding steps, presumably due to the length of the purification protocol.

Table S6. Oligomeric structure of KDO8PS.

Protein standards and KDO8PS molecular weights and elution volumes on a Superose 12 10/300 GL size exclusion column.

Protein ID	Molecular Weight (kDa)	V_e/V_0
Blue dextran 200	2000	1.00
Ferritin	440	1.27
catalase	232	1.43
Aldolase	158	1.47
$KDO8PS_{wt}$	123 ± 3	1.51
$KDO8PS_{H6}$	120 ± 13	1.52
Ovalbumin	45	1.64
Ribonuclease	13.7	1.94

Figure S5. Amino acid sequence alignment of KDO8PSs and DAHPS.

Amino acid sequences of metal-dependent and -independent KDO8PSs, plus *E. coli* DAHPS(Phe). The metal-dependent KDO8PSs were from *C. jejuni*, *Helicobacter pylori*, *Aquifex aeolicus,* and the metal-independent KDO8PS was from *E. coli*. The conserved metal-binding residues are highlighted in cyan. The green-highlighted K is presumed general acid catalyst in THI breakdown. Numbers in brackets (e.g., [13]) indicate the number of amino acids left out of the alignment figure to save space. The Genbank accession numbers are: *C. jejuni* KDO8PS – EFV08406.1, *H. pylori* KDO8PS – AAD05587.1, *A. aeolicus* KDO8PS – O66496.1; *E. coli* KDO8PS – P0A715.1, *E. coli* DAHPS(Phe) – P0AB92.

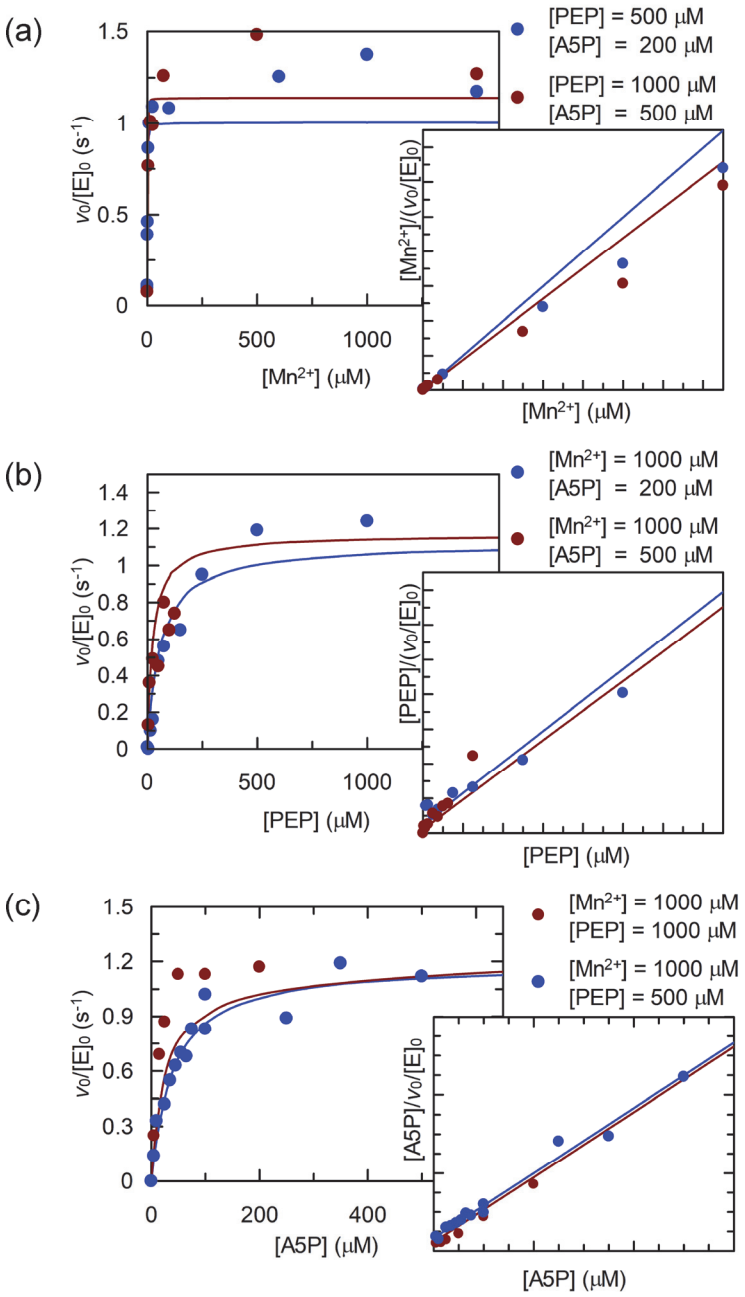

Figure S6. Kinetic parameters for KDO8PS$_{H6}$.

Kinetic constants for KDO8PS$_{H6}$ with rapid equilibrium sequential ordered ter ter kinetic mechanism. Initial velocity vs. [substrate] plots for: (a) Mn^{2+}, (b) PEP, and (c) A5P fitted to equation **1**, **1a.** The inset graphs are Hanes plots, [S]/(v_0/[E]$_0$) vs. [S].

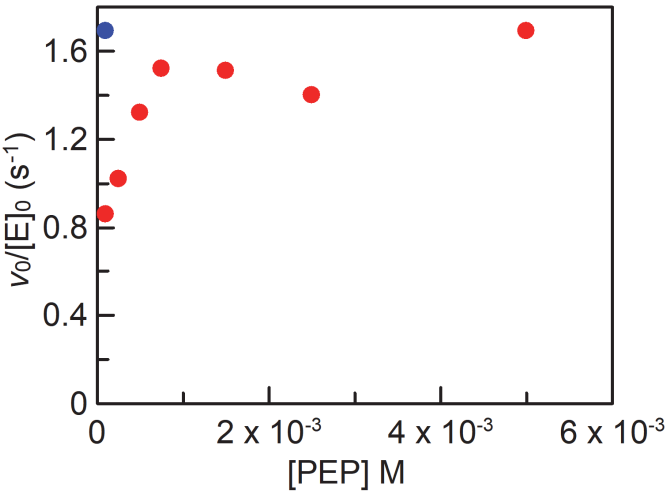

Figure S7. KDO8P oxime mode of inhibition of with respect to PEP.

$KDO8PS_{wt}$ activity was measured in the presence of 500 μM KDO8P oxime and increasing concentrations of PEP. Increasing [PEP] outcompeted KDO8P oxime, as the activity of the inhibited $KDO8PS_{wt}$ (red dots) returned to the control activity (no KDO8P oxime, blue dot) at higher [PEP].

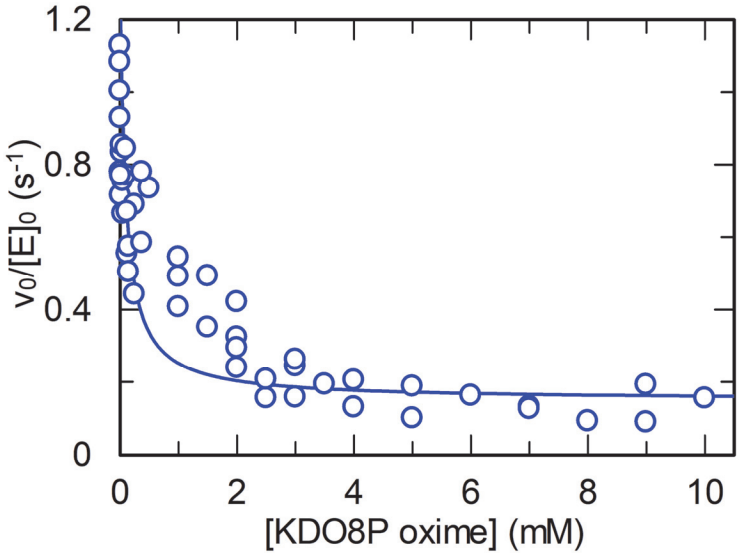

Figure S8. Fast-binding inhibition of $KDO8PS_{H6}$ by KDO8P oxime.

K_i = 10 ± 2 μM, with 9% residual rate.

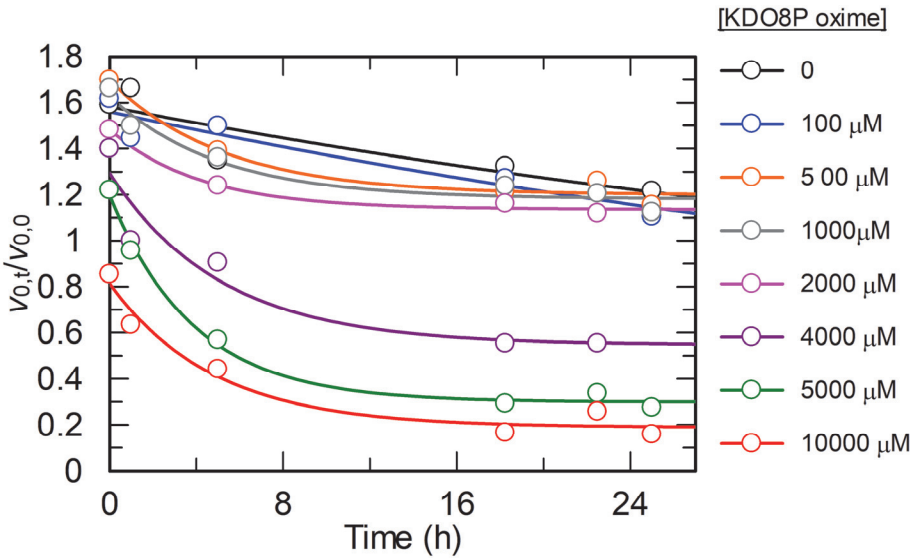

Figure S9. Rate of onset of slow-binding inhibition (k_{obs}) of KDO8PS$_{wt}$ as a function of [KDO8P oxime].

Residual rate ($v_{0,t}/v_{0,0}$) versus incubation time for varying [KDO8P oxime] was fitted to equation **7** to derive k_{obs} at each inhibitor concentration. The k_{obs} values were used directly in equation **8** (Figure 8) to fit $k_{on,conc}$ and $k_{off,conc}$. There was enzyme inactivation when [I] = 0, presumably due to enzyme denaturation, characterized by $k_{denaturation}$ = 0.011 h^{-1}. In contrast there was no continued loss of activity at high [I] and long incubation times, implying that the inhibitor stabilized the enzyme. Therefore, it was not clear whether $k_{denaturation}$ should be subtracted from k_{obs}. Subtracting $k_{denaturation}$ and fitting the new k_{obs} values to equation **8** yielded $k_{off,conc}$ = (0.9 ± 5.2) × 10^{-4} h^{-1}, or t_R = 80 days to ∞. The corresponding analysis for KDO8PS$_{H6}$, where the treatment of $k_{denaturation}$ was more clearcut, yielded $k_{off,conc}$ = 0.016 h^{-1}, in good agreement with the more conservative treatment of the wild type data, where $k_{off,conc}$ = 0.014 h^{-1} (Figures S10 – S12). This supported the more conservative treatment of the KDO8PS$_{wt}$ data.

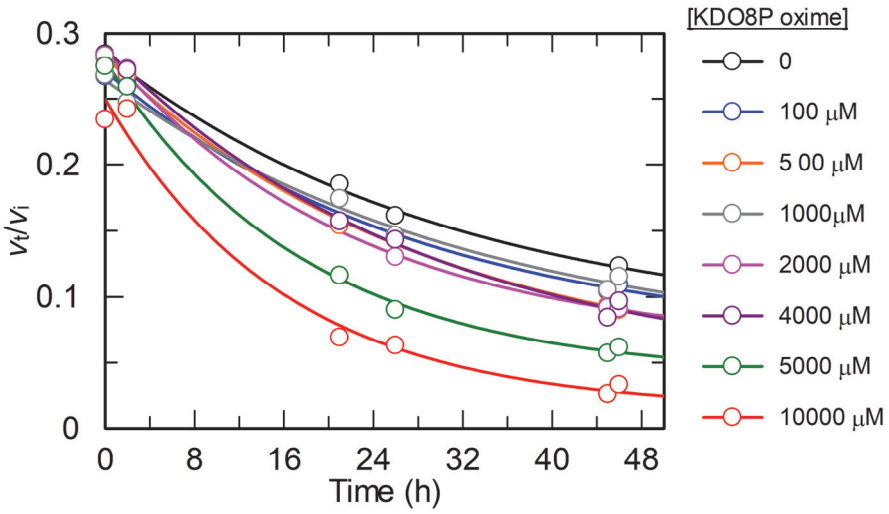

Figure S10. Rate of onset of slow-binding inhibition (k_{obs}) of KDO8PS$_{H6}$ as a function of [KDO8P oxime].

For the His_6-tagged enzyme, residual rate ($v_{0,i}/v_{0,0}$) versus incubation time for varying [KDO8P oxime] was fitted to equation **7** to derive k_{obs} at each inhibitor concentration. Unlike $KDO8PS_{wt}$, the rate of inactivation when [I] = 0, $k_{denaturation}$, was significant, and was subtracted from k_{obs} for other inhibitor concentrations.

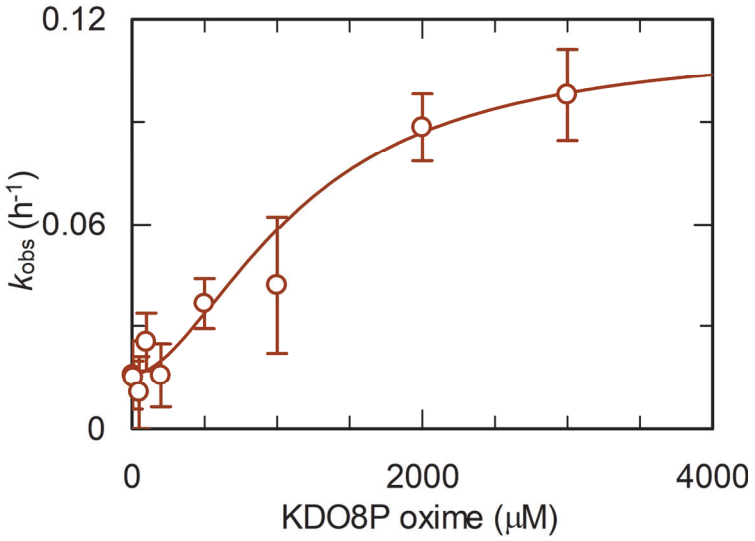

Figure S11. Rate of onset of slow-binding inhibition (k_{obs}) of $KDO8PS_{H6}$ as a function of [KDO8P oxime].

The k_{obs} values from Figure S10 were fitted versus [KDO8P oxime] (eq. **8**). $k_{on,conc}$ = 0.10 ± 0.01 h^{-1}, $k_{off,conc}$ = 0.016 ± 0.002 h^{-1}, with the Hill coefficient fixed at 1.8 (see Figure S12).

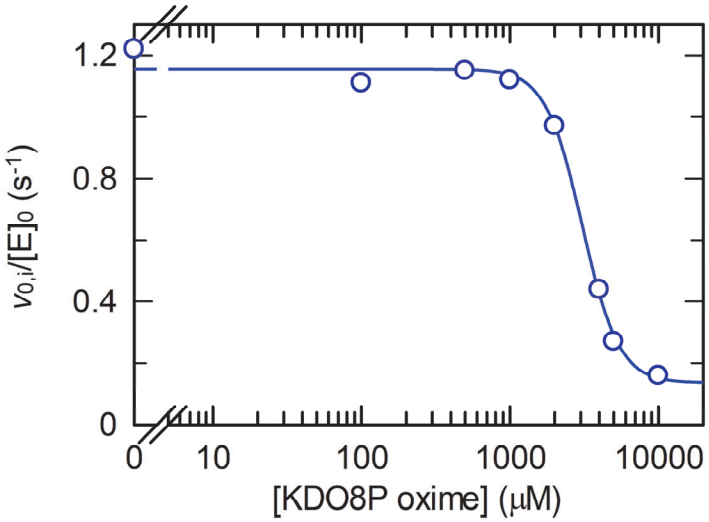

Figure S12. Concentration dependence of slow-binding inhibition of $KDO8PS_{H6}$ after 46 h preincubation.

Initial velocities were fitted to equation **9**. IC_{50} = 590 ± 110 μM, n = 1.8 ± 0.5. The Hill coefficient was lower than for wild type enzyme, 3.5, but still exhibited cooperativity. Inhibitor concentrations are those in the preincubation mixture, before dilution into the assay mixture.